Confirmation of Zero-N Behavior in a High Gain Grid Structure at Millimeter-Wave Frequencies

Steven J. Franson, *Senior Member, IEEE*, and Richard W. Ziolkowski, *Fellow, IEEE*

***Abstract*—A multilayer grid structure that has been used previously to create an antenna with high directivity and gain and that has been explained as having a near zero index of refraction is extended to millimeter-wave frequencies. Alternate explanations for the associated phenomena are examined. Further confirmation of this "zero-n" behavior is presented.**

***Index Terms*—Antennnas, metamaterials, millimeter waves, zero-n.**

I. Introduction

RESEARCH results on directive antennas obtained by augmenting a basic antenna with combinations of metamaterial substrates and superstrates have been reported, for example, in [1]–[10]. These metamaterial-enhanced antennas, such as the one illustrated in Fig. 1, have the potential to achieve high directivity; and, hence, they have a high potential for use in many communication systems. Of particular interest within the millimeter-wave spectrum are the applications to automotive radar, broadband point-to-point communications, and millimeter-wave imaging. Enoch *et al.* [1] have shown how a simple stack of metallic grids can lead to *ultra-refraction* [11], [12]. Because the resulting metamaterial structure has an index of refraction, n, which is positive, but less than one and near zero, all of the rays emanating from a point source within such a slab of "zero-n" material would refract, by Snell's Law, almost parallel to the normal of every radiating aperture. A variety of other interesting effects occur as the index approaches zero and a zero-n type of metamaterial is realized, e.g., see [13]–[18]. Despite general agreement on the zero-n interpretation for the enhanced directivity behavior, alternative explanations for the properties of the finite periodic structure defining the metamaterial, such as that discussed in [19], have been given. We will consider the metamaterial grid structure shown in Fig. 1 at millimeter-wave frequencies and will confirm that it does indeed exhibit a zero-n behavior.

Manuscript received February 01, 2008; revised June 16, 2008. First published July 25, 2008; current version published May 20, 2009. The work of R. W. Ziolkowski was supported in part by DARPA under Contract HR0011-05-C-0068.

S. J. Franson was with Millimeter-Wave Research, Motorola Labs, Tempe, AZ 85284 USA. He is now with Microwave Systems Solutions, Crane Electronics Group, Chandler, AZ 85226 USA (e-mail: Steve.Franson@crane-eg.com).

R. W. Ziolkowski is with the Department of Electrical and Computer Engineering, University of Arizona, Tucson, AZ 85721 USA (e-mail: ziolkowski@ece.arizona.edu).

Color versions of one or more of the figures in this letter are available online at http://ieeexplore.ieee.org.

Digital Object Identifier 10.1109/LAWP.2008.2002807

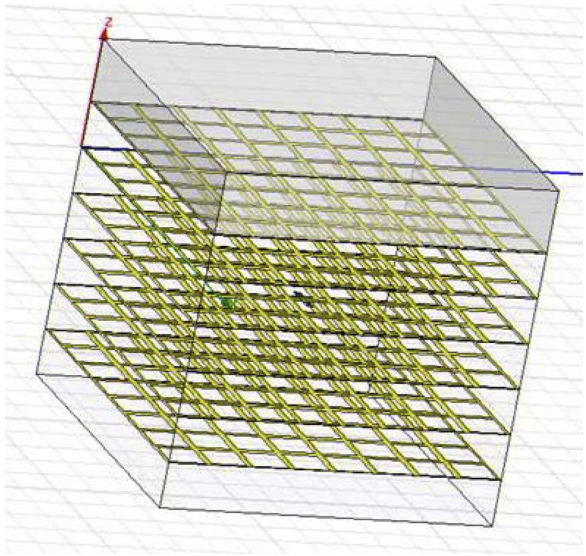

Fig. 1. "Zero-n" antenna structure: a dipole radiating in the presence of a multilayer, $8 \times 8 \times 6$ grid structure.

II. Grid Structure at Millimeter-Wave Frequencies

The authors have demonstrated experimentally that a two-layer version of the grid structure shown in Fig. 1 integrated with a patch antenna at 60 GHz leads to enhanced directivity; can transmit data rates over 2 Gb/s, and hence, may be useful for millimeter-wave communications systems. At millimeter-wave frequencies, the loss associated with any substrate is of utmost concern in the design process. Ideally, one would like to construct a millimeter-wave structure only out of metal, with air spacing in between. Since this is not conducive to high volume manufacturing of any structure, a suitable substrate that met all of the design constraints was found. It was a foam material which is purchased in sheets that are nearly 40 mils thick (approximately 1 millimeter), have copper cladding on one side, and have a peel off adhesive on the other. Because the substrate is filled with air pockets, its properties are fairly close to air, its relative permittivity being equal to 1.5, a value slightly over 1. Moreover, its loss tangent is a very low value for millimeter-wave frequencies, being equal to 0.001. Consequently, we were able to easily have metallic lines patterned on the material and have several layers attached together to form a stack.

A CST Microwave Studio unit cell model of the grid structure was constructed to determine its permittivity and permeability properties. Each of the physically realized grid layers had the dimensions: 5-mil line widths, 2-mil metal thickness, and a 70-mil period, while the separation between each grid layer was 39 mils. As a result, the unit cell model was a square PEC-PMC

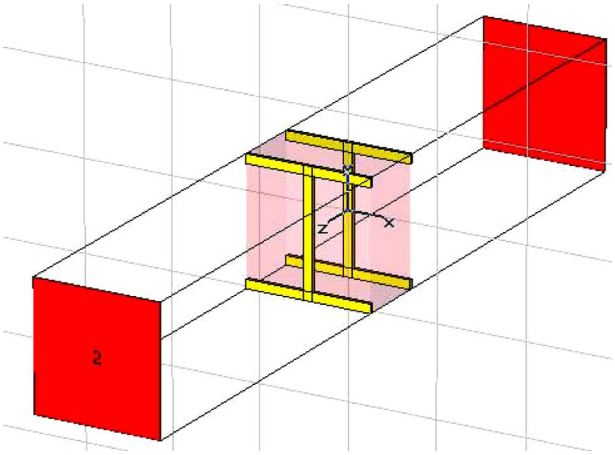

Fig. 2. The CST model of the 2-layer grid unit cell.

waveguide (normally incident plane wave with its electric (magnetic) field orthogonal to the PEC (PMC) side-walls of the waveguide), having wave-ports on each of its ends. The two grid layer structure, which has a 43-mil thickness, was centered about the middle of the 70-mil square waveguide. Because of the symmetries provided by the PEC and PMC side-walls, the actual form of the unit cell is the two "I" pattern shown in Fig. 2. The model represents a 2-layer infinite grid slab. The CST simulations were run with a total of 58,080 hexahedral mesh cells, the maximum mesh cell size being 3.83 mils. The accuracy was set to -60 dB. Two passes achieved a delta S equal to 0.01; the solve time was 90 s.

III. Parameter Extraction

A parameter extraction routine was developed and used to determine the permittivity and permeability of the grid structure from the CST-predicted reflection and transmission (S-parameter) data. Like all of the extraction codes reported in the literature, e.g., [21]–[24], this routine was based on the NWR approach given in [25] and [26] was implemented as in [27]. The code had no prior knowledge on whether the material was electric or magnetic, negative or positive. It simply took the S-parameter data obtained by scattering a plane wave from a thin slab of the material under test and then extracted the effective material parameters of that slab. The extraction can be very difficult, especially for thick samples, where multiple solutions can exist.

Because of some lingering controversy in the metamaterials community concerning this extraction process (the imaginary part of the extracted nondominant material component can exhibit active properties in the resonance region), we carefully validated our routine with a canonical electric and magnetic Lorentz medium slab. The relative material parameters of this slab were defined by the expressions implemented in the CST simulation environment as follows:

$$\varepsilon_r(\omega) = \varepsilon_\infty + \frac{\omega_{0,e}^2(\varepsilon_{DC} - \varepsilon_\infty)}{-\omega^2 + j\delta_e\omega + \omega_{0,e}^2}$$
$$\mu_r(\omega) = \mu_\infty + \frac{\omega_{0,m}^2(\mu_{DC} - \mu_\infty)}{-\omega^2 + j\delta_m\omega + \omega_{0,m}^2} \quad (1)$$

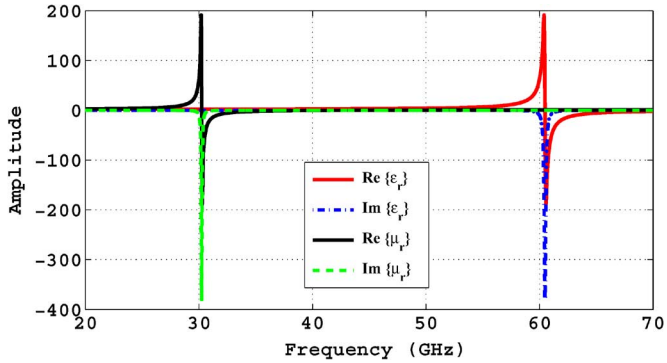

Fig. 3. Electric and magnetic Lorentz material responses of the canonical slab used to validate the extraction routine.

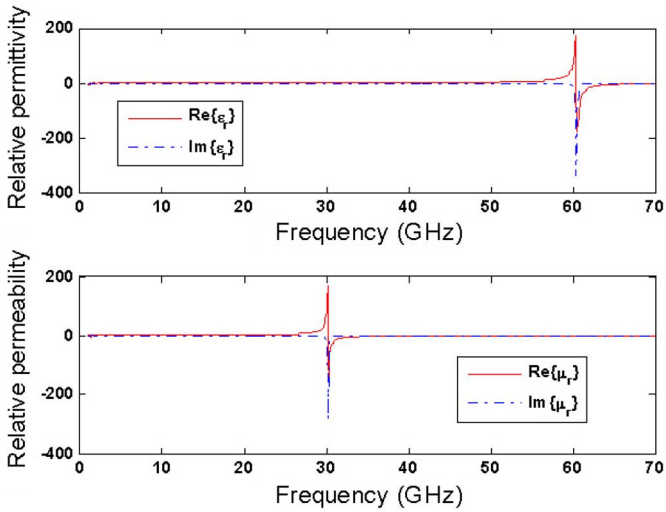

Fig. 4. Constitutive parameters extracted from the CST calculated S-parameters when a normally incident plane is scattered from the canonical Lorentz-material slab.

where $\omega_{0,e} = 380 \times 10^9$, $\delta_e = 1.0 \times 10^9$, $\varepsilon_\infty = \mu_\infty = 1.0$, $\varepsilon_{DC} = \mu_{DC} = 2.0$, $\omega_{0,m} = 190 \times 10^9$, $\delta_m = 0.5 \times 10^9$. As Fig. 3 shows, the resulting relative material parameters have electric and magnetic resonances at different frequencies and with different bandwidths.

The calculated S-parameters were then imported into the parameter extraction code (implemented in MATLAB). As expected, without paying careful attention to the thickness of the slab, the extraction routine would generate some positive values for the nonresonant component. However, if the slab thickness was restricted to produce less than a pi-phase shift across the slab, the extraction routine always produced the correct signs for the imaginary parts of the relative material parameters. Because the analytical models exhibit very large responses at the resonance, i.e., large magnitudes of the permittivity or permeability, the thickness of the slab had to remain small. For a 1.0-mil-thick Lorentz-material slab, the outputs of the extraction code for the relative permittivity and permeability are shown in Fig. 4. This test case demonstrates that if used properly, the parameter extraction code can produce good quality results, and can distinguish between the electric and magnetic resonances.

The CST calculated S-parameters of the unit cell of the proposed 2-layer grid structure shown in Fig. 2 were examined next

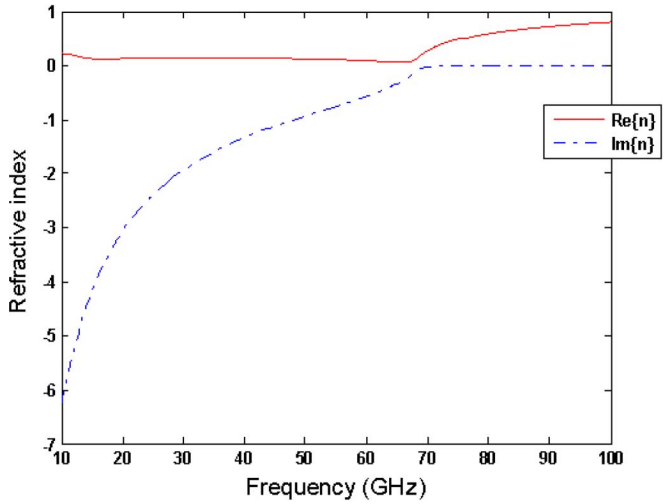

Fig. 5. The extracted index of refraction of the two-layer grid structure.

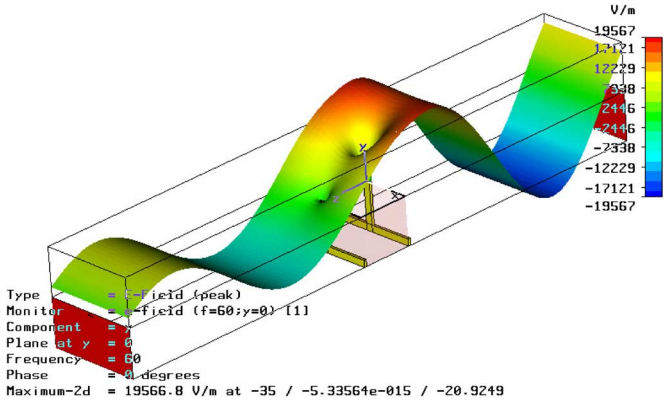

Fig. 6. The transmitted electric field distribution calculated with CST for the 2-layer grid structure.

to test whether or not the extracted constitutive parameters coincided with the anticipated zero-n behavior. The phase across the effective slab was calculated to ensure that it was unique, i.e., that it did not cross over into the next 2π interval. The corresponding extracted relative permittivity and permeability values exhibited only passive responses. The resulting extracted index of refraction is shown in Fig. 5. It remains imaginary at lower frequencies, and then starts to have positive values that rise from zero after the plasma frequency. In particular, we note that while it may appear as if the unit cell was a version of the CLS-based (capacitively loaded strip-based) metamaterial structure considered in [22], the arms of the "I" inclusions are actually touching the side-walls of the waveguide. In fact, the grid structure is actually an extreme version of that CLS-based metamaterial, where the resonance frequency goes to zero and the relative DC permittivity goes to infinity because the gap size goes to zero (which causes the quasi-static capacitance to go to infinity). From a related point of view, the CLS-based material has an effective inductance, L, and capacitance, C, so that its resonance frequency is specified as

$$\omega_0 = 1/\sqrt{LC}. \tag{2}$$

As the gap distances between the CLS inclusions decrease, the capacitances between the elements increase. As a result, the angular resonance frequency, ω_0, gets closer to zero. In the limit, where the gap sizes become zero, the resonant frequency is equal to zero. Consequently, the grid structure creates an effective medium whose index of refraction satisfies a Lorentz model with a zero resonance frequency, i.e., it can be described by the Drude model

$$n_{eff}^2(\omega) = 1 - \frac{\omega_p^2}{\omega^2 + j\delta_e\omega} \tag{3}$$

where ω_p is the angular plasma frequency. This Drude model of the index of refraction recovers the behavior shown in Fig. 5. The plasma frequency and, hence, the zero-n behavior occurs at the desired operating frequency, 60 GHz.

IV. Phase Progression

The grid structure is actually a well known low frequency filter structure that has a well-known example, i.e., the screen on the window of a microwave oven, which passes visible light, but contains the microwave radiation. This behavior is captured by the effective permittivity and, hence, the effective index of refraction described by the Drude model (3). The ability of periodic arrangements or wires or metallic traces to create artificial plasmas is well-known [28], [29]. The Drude model for the permittivity also predicts a negative permittivity for frequencies below the plasma frequency. When the permittivity is negative and the permeability is the same as free space, only evanescent (exponentially decaying) waves exist in such an epsilon-negative (ENG) medium. Additionally, immediately above the plasma frequency, the index of refraction can be between 0 and 1; and, as a result, this frequency interval is also known as the *ultra-refraction* [12] region. However, at these higher frequencies, the structure may not be small in comparison to the free-space wavelength. Consequently, the zero-n interpretation could be questioned in this portion of the frequency spectrum, i.e., the unit cell may not be small enough to correctly claim the structure acts as an effective homogenous medium with zero-n properties. Similarly, there have also been questions raised, for instance in [19], as to whether or not the zero-n behavior is the correct interpretation. The grid structure could be acting simply as a two dimensional grating with a high diffraction efficiency at zero order. We believe that our simulation results provide further evidence that the zero-n explanation captures the correct physical behavior of the two-layer grid structure.

If such a grid structure does indeed have an index of refraction that is close to zero, then the phase progression through it should be extremely slow. This means that there should be an almost static phase distribution within the structure and that the phase at the exit face of the 2-layer grid structure should be nearly equal to its value at the entrance face. In Fig. 6 the CST-predicted electric field of the wave propagating through it is shown. A one-dimensional plot of this electric field along

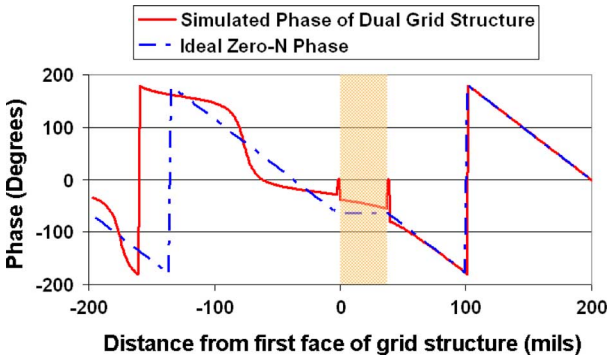

Fig. 7. One dimensional plot showing a comparison of the phase term calculated for the 2-layer grid structure and for the ideal zero-n material slab.

the center of the simulation space was obtained; it is shown in Fig. 7. In the region before the structure, the phase term results from the behavior of the incident and reflected fields. On the other hand, the fields beyond the grid structure contain only information about the transmitted wave. Therefore, the phase term immediately after the structure should be compared to an ideal case which assumes a zero phase accumulation through the material. As Fig. 7 shows, the phase at a short distance beyond the structure matches that found for the ideal case of a zero-n medium. Therefore, we have confirmed even further that such a grid structure has an effective index of refraction close to zero.

V. Conclusion

In conclusion, we have raised questions as to the validity of describing the grid structure as a zero-n material, and have supplied additional evidence in an attempt to answer those questions. Our results clearly show that the parameter extraction predicts a zero-n response for the 2-layer grid structure. Also, when examining the phase progression through this metamaterial, it exhibits zero-n behavior. In particular, the phase of the wave transmitted through the 2-layer grid metamaterial has the same phase as if it had propagated through an ideal near zero-n material.

References

[1] S. Enoch, G. Tayeb, P. Sabouroux, N. Guérin, and P. Vincent, "A metamaterial for directive emission," *Phys. Rev. Lett.*, vol. 89, p. 213902, 2002.

[2] B.-I. Wu, W. Wang, J. Pacheco, X. Chen, T. Grzegorczyk, and J. A. Kong, "A study of using metamaterials as antenna superstrate to enhance gain," *Progr. In Electromagn. Res.*, vol. PIER 51, p. 295328, 2005.

[3] A. R. Andrew, K. P. Esselle, B. C. Sanders, and T. S. Bird, "High-gain 1D EBG resonator antenna," *Microw. Opt. Technol. Lett.*, vol. 47, pp. 107–114, Oct. 2005.

[4] A. Ourir, A. de Lustrac, and J.-M. Lourtioz, "All-metamaterial-based subwavelength cavities ($\lambda/60$) for ultrathin directive antennas," *Appl. Phys. Lett.*, vol. 88, p. 084103, February 2006.

[5] E. Saenz, I. Ederra, R. Gonzalo, and P. de Maagt, "Enhancement of the power radiated by a dipole antenna at boresight by means of a left handed superstrate," in *Proc. IEEE Int. Workshop on Antenna Technol. Small Antennas and Novel Metamater. IWAT2006*, White Plains, NY, Mar. 6–8, 2006, pp. 9–12.

[6] Y. Lee, W. Park, J. Yeo, and R. Mittra, "Directivity enhancement of printed antennas using a class of metamaterial superstrates," *Electromagn.*, vol. 26, pp. 203–218, 2006.

[7] Y. Vardaxoglou and F. Capolino, "Review of highly-directive flat-plate antenna technology with metasurfaces and metamaterials," in *Proc. 36th Eur. Microw. Conf.*, Manchester, UK, Sep. 2006, pp. 963–966.

[8] Z.-B. Weng, N.-B. Wang, Y.-C. Jiao, and F.-S. Zhang, "A directive patch antenna with metamaterial structure," *Microw. Opt. Technol. Lett.*, vol. 49, pp. 456–459, February 2007.

[9] P. M. T. Ikonen, E. Saenz, R. Gonzalo, and S. A. Tretyakov, "Modeling and analysis of composite antenna superstrates consisting on grids of loaded wires," *IEEE Trans. Antennas Propag.*, vol. 55, pp. 2692–2700, Oct. 2007.

[10] H. Xu, Z. Zhao, Y. Lv, C. Du, and X. Luo, "Metamaterial superstrate and electromagnetic band-gap substrate for high directive antenna," *Int. J. Infrared Millimet. Waves*, vol. 29, pp. 493–498, 2008.

[11] G. Tayeb, S. Enoch, P. Vincent, and P. Sabouroux, "A compact directive antenna using ultrarefractive properties of metamaterials," in *Proc. Int. Conf. on Electromagn. Adv. Applicat., ICEAA'03*, Torino, Italy, Sep. 08–12, 2003, pp. 423–426.

[12] D. R. Maystre, S. Enoch, and G. Tayeb, "Ultrarefraction and negative refraction in metamaterials," *Proc. SPIE*, vol. 5359, p. 64, 2004.

[13] R. W. Ziolkowski, "Propagation in and scattering from a matched metamaterial having a zero index of refraction," *Phys. Rev. E*, vol. 70, p. 046608, Oct. 2004.

[14] A. Alù and N. Engheta, "Achieving transparency with plasmonic and metamaterial coatings," *Phys. Rev. E*, vol. 72, p. 016623, 2005.

[15] J. B. Pendry, D. Schurig, and D. R. Smith, "Controlling electromagnetic fields," *Science*, vol. 312, pp. 1780–1782, 2006.

[16] A. Alù, M. G. Silveirinha, A. Salandrino, and N. Engheta, "Epsilon-near-zero metamaterials and electromagnetic sources: Tailoring the radiation phase pattern," *Phys. Rev. B*, vol. 75, p. 155410, 2007.

[17] B. Edwards, A. Alù, M. E. Young, M. Silveirinha, and N. Engheta, "Experimental verification of epsilon-near-zero metamaterial coupling and energy squeezing using a microwave waveguide," *Phys. Rev. Lett.*, vol. 100, p. 033903, Jan. 2008.

[18] R. Liu, Q. Cheng, T. Hand, J. J. Mock, T. J. Cui, S. A. Cummer, and D. R. Smith, "Experimental cemonstration of electromagnetic tunneling through an epsilon-near-zero metamaterial at microwave frequencies," *Phys. Rev. Lett.*, vol. 100, p. 023903, Jan. 2008.

[19] Y. C. Huang, J. S. Lih, J. L. Chern, and E. Li, "Grating-like interpretation of the meta-material using in directive emission," in *Proc. Progr. In Electromagn. Res. Symp.*, Honolulu, HI, Oct. 13–16, 2003, p. 16.

[20] S. J. Franson and R. W. Ziolkowski, "Gigabit per second data transfer in high gain metamaterial structures at 60 GHz," *IEEE Trans. Antennas Propag.*, 2009, to be published.

[21] D. R. Smith, S. Shultz, P. Markos, and C. M. Soukoulis, "Determination of effective permittivity and permeability of metamaterials from reflection and transmission coefficients," *Phys. Rev. B*, vol. 65, p. 195104, April 2002.

[22] R. W. Ziolkowski, "Design, fabrication, and testing of double negative metamaterials," *IEEE Trans. Antennas Propag.*, vol. 51, no. 7, pp. 1516–1529, Jul. 2003.

[23] X. Chen, T. Grzegorczyk, B.-I. Wu, J. Pacheco, Jr., and J. A. Kong, "Robust method to retrieve the constitutive effective parameters of metamaterial," *Phys. Rev. E*, vol. 70, p. 016608, Jul. 2004.

[24] D. R. Smith, D. C. Vier, T. Koschny, and C. M. Soukoulis, "Electromagnetic parameter retrieval from inhomogeneous metamaterials," *Phys. Rev. E*, vol. 71, p. 036617, Mar. 2005.

[25] A. M. Nicolson and G. F. Ross, "Measurement of the intrinsic properties of materials by time domain techniques," *IEEE Trans. Instrum. Meas.*, vol. IM-19, p. 377382, Nov. 1970.

[26] W. B. Weir, "Automatic measurement of complex dielectric constant and permeability at microwave frequencies," *Proc. IEEE*, vol. 62, p. 3336, Jan. 1974.

[27] P. Imhof, "Metamaterial-based epsilon-negative (ENG) media: Analysis and designs," EPFL Masters thesis, Lausanne, Switzerland, Mar. 2006.

[28] W. Rotman, "Plasma simulation by artificial dielectrics and parallel-plate media," *IEEE Trans. Antennas Propag.*, vol. 10, pp. 82–95, Jan. 1962.

[29] J. B. Pendry, A. J. Holden, W. J. Stewart, and I. Youngs, "Extremely low frequency plasmons in metallic mesostructures," *Phys. Rev. Lett.*, vol. 76, pp. 4773–4776, Jun. 1996.